Check for updates

AJAE

Open Access

Vol. 16, No. 2, 2021146, June 2022
doi: https://doi.org/10.5572/ajae.2021.146
ISSN (Online) 2287-1160, ISSN (Print) 1976-6912

Research Article

COVID-19 Lockdown: Impact on PM_{10} and $PM_{2.5}$ in Six Megacities in the World Assessed Using NASA's MERRA-2 Reanalysis

Sara Said[1)], **Zeinab Salah**[1)], **Ibrahim Abdelmageid Hassan**[2),4),*], **Mohamad Magdy Abdel Wahab**[3),4)]

[1)]Egyptian Meteorological Authority, 11784, Cairo, Egypt
[2)]Faculty of Science, Alexandria University, 21511, Moharem Bay, Alexandria, Egypt
[3)]Department of Meteorology, Faculty of Science, Cairo University, 12613, Giza, Egypt
[4)]National Scientific Committee for Problems in Environment (SCOPE), Academy of Scientific Research & Technology (ASRT), 101 Kasr Al-Ini Street, Cairo, Egypt

***Corresponding author.**
Tel: +00201227173094
E-mail: ihassan2006@gmail.com/ Ibrahim.abdelmaged@alexu.edu.eg

Received: 8 December 2021
Revised: 20 February 2022
Accepted: 13 April 2022

ABSTRACT The changes in air quality were investigated in six megacities during the shutdown phases in 2020 and were compared to the same time periods in the previous 10 years (2010–2019) using the data of Modern-Era Retrospective Analysis and Research and Application, version 2 (MERRA-2). The concentrations of PM_{10} and $PM_{2.5}$ were greatly reduced in all megacities during the lockdown in 2020 when compared to the same period in 2019 and in the previous ten years. The highest reduction in PM_{10} was recorded in Delhi, and São Paulo (21%, and 15% and by 27%, and 9%), when compared with the concentrations in 2019 and in the period 2010–2019, respectively. Similarly, levels of $PM_{2.5}$ in Delhi, São Paulo, Beijing, and Mumbai decreased by 20%, 14%, 12%, and 10%, respectively in 2020 when compared to the last ten years. Results indicated that the lockdown is an effective mitigation measure to improve air quality. The MERRA-2 reanalysis dataset could be a vital tool in air quality studies in places with a lack of In-situ observations.

KEY WORDS Satellite observation, MERRA-2, COVID-19, Lockdown, Megacities, Air quality, PM_{10}, $PM_{2.5}$

1. INTRODUCTION

A massive number of viral infection cases were reported at the beginning of December 2019 in Wuhan city of China (Lu *et al.*, 2020), which was identified as a coronavirus on December 31, 2019 (WHO, 2020a). The virus kept on spreading across the whole world covering all countries. On February 2020 WHO declared the disease as Pandemic and named it COVID-19 (Bashir *et al.*, 2020; Bera *et al.*, 2020; Shi and Brasseur, 2020; WHO, 2020a, b, c). WHO announced some measures to contain the COVID-19 pandemic such as isolation, home quarantine, social distancing, restriction of transportation (domestic national, and international), and the lockdown (Rohrer *et al.*, 2020). All countries around the globe enforced lockdown to contain COVID-19 pandemic, which resulted in improving of air quality, as a consequence of reducing local pollutant emissions, particularly in the highly populated cities (Ismail *et al.*, 2021; Luna *et al.*, 2018).

Chronic exposure to atmospheric contamination may represent an encouraging context for the spread of the new virus and there is a significant correlation between air-quality data and infected cases of the COVID-19 (Fattorini and Regoli, 2020). Bauwens *et al.* (2020) stated that lockdown and reductions in human activities positively affected the environment in China and Western Europe. These findings were supported by similar studies in India (Chhikara and Kumar, 2021; Gupta *et al.*, 2020), the USA (Bashir *et al.*, 2020) and, recently, in Egypt (Abou El-Magd and Zanaty, 2021; El-Sheekh and Hassan, 2021).

Air pollution is a serious problem as it poses a major threat to human health, causing an increased mortality rate and premature deaths (Bera *et al.*, 2020; WHO, 2020b; Haque and Singh, 2017). Cosmopolitan megacities suffer from poor air quality that does not meet WHO guidelines (e.g. Gupta *et al.*, 2020; Haiba and Hassan, 2018; Basahi *et al.*, 2017; WHO/UNEP, 1994). The most polluted megacities that are facing high levels of air pollution are Cairo (Egypt), Delhi, Mumbai (India), Beijing (China), Tehran (Iran), and São Paulo (Brazil) (Bauwens *et al.*, 2020; WHO/UNEP, 1994). These cities are characterized by high concentrations of Particulate Matter (PM_{10} and $PM_{2.5}$), carbon monoxide (CO), nitrogen oxides (NO_x), sulfur dioxide (SO_2), and ground-level ozone (O_3) (Abou El-Magd and Zanaty, 2021; El Sheekh and Hassan, 2021; Bauwens *et al.*, 2020; Mostafa *et al.*, 2018; Olivieri and Scoditti, 2005).

The current study aims to assess the effects of reduced activity resulting from the spread of the COVID-19 on PM_{10} and $PM_{2.5}$ concentrations in six major cities around the world, namely: Cairo, Delhi, Mumbai, São Paulo, Beijing, and Tehran, all of which are major epicenters of the outbreak. To achieve this goal, we used time series of aerosol concentrations extracted from Modern-Era Retrospective Analysis, Research and Application, Version 2 (MERRA-2) to see how the particulate matter concentrations in these cities vary during the year using the long time series available from MERRA2. In addition to determining how the reduction of the anthropogenic activities because of the lockdown has been captured by MERRA-2.

2. DATA AND METHODOLOGY

2. 1 Study Megacities

Cairo, the capital of Egypt, (30°2′N, 31°14′E) is a large metropolitan city with a population of about 21 million (Table 1). It has a high level of air pollution due to the rapid increase in urbanization and industrialization (Abou El-Magd and Zanaty, 2021; Abou El-Magd *et al.*, 2020; Mostafa *et al.*, 2018). On 14 February 2020, the Egyptian government announced the first cases of Corona in the country, and by 19 March 2020, several protective steps were announced, including a partial curfew from 7 PM until 6 AM all over Egypt, along with reducing the number of employees. The suspension of studies in all governorates and the closure of places of worship, public parks, cafes, restaurants, shopping centres, and entertainment places, in addition to the complete closure on the Easter holidays on April 20, and Eid al-Fitr (May 23–25, 2020).

Table 1. The studied megacities, their countries and their latitudes and longitudes that used to extract the MERRA-2 data.

Megacity	Country	Latitude	Longitude
Cairo	Egypt	30.08	31.29
Delhi	India	28.38	77.13
Mumbai	India	19.08	77.13
Beijing	China	39.54	116.23
Tehran	Iran	35.70	51.35
São Paulo	Brazil	−23.32	−46.37

Delhi is the capital of India and is located in the north of India (28°36′36″N, 77°13′48″E), with a population of about 31 million. Mumbai is the financial, commercial, and entertainment capital of India and it lies on the west coast of India (19°07′60″N, 72°87′77″E), with a population exceeded 20 million (Table 1). (https://worldpopulationreview.com/world-cities/). The main sources of air pollution in India are vehicle exhaust, road dust, waste burning, industrial activities, oil combustion, and coal production (Chhikara and Kumar, 2021; Gupta *et al.*, 2020). Indian government enforced the full lockdown from March 25 to April 14, 2020 as the COVID-19 was expanded vigorously (Dhaka *et al.*, 2020).

Beijing is the capital of China and lies in the north region of China (39°90′42″N, 116°40′74″E), with a population of about 22 million. The coronavirus was first broke out in Wuhan in December 2019, therefore, the Chinese government had taken unprecedentedly stringent steps around the country to contain the spread of the pandemic. China has cut off Wuhan from other areas on January 23, 2020 (Pei *et al.*, 2020). Industry and manufacturing remained very limited in Beijing until March, and large-scale production and transportation activities did not resume until late April.

Tehran is Iran's capital and most overcrowded city in Iran (35°68′92″N, 51°38′90″E), its population is about 10 Million. Tehran has faced high levels of PM_{10} and $PM_{2.5}$ due to several industrial activities and the transportation of over 4 million vehicles in the city (Hosseini and Shahbazi, 2016). The first novel case of coronavirus was announced in mid-February 2020 in Iran, which has been accompanied by reinforcing the lockdown in many cities in Iran, including Tehran, to contain the COVID-19 (Faridi *et al.*, 2020).

São Paulo is located 60 kilometers from Brazil's southeast coast (23°55′05″S, 46°63′33″W) at approximately 800 m above the sea level (Molina *et al.*, 2004), and it is the largest metropolitan area in Brazil with 23 million, which constitutes about 20% of the total population of Brazil (Doraiswamy *et al.*, 2017). The first case of COVID-19 was recorded on March 24, 2020 in São Paulo; therefore, the state government ordered a partial lockdown. Air quality in São Paulo metropolitan region and São Paulo city was more influenced by industrial sources (Nakada and Urban, 2020).

Table 1 contains the latitudes and longitudes of the six megacities and the selected months of the lockdown in every city.

2.2 MERRA-2 Product

Modern-Era Retrospective Analysis and Research and Application, version 2 (MERRA-2) is produced by the NASA Global Modelling and Assimilation Office (GMAO), and it is the first satellite-era global atmospheric reanalysis to assimilate space-based observations of aerosols and represent their interactions with other physical processes in the climate change studies because of its continuous spatial and temporal high-quality resolutions (Delgado-Bona *et al.*, 2020; Bosilovich *et al.*, 2019; Randles and da Silva, 2017), in addition to its usage in many studies related to the particulate matter in different regions in the world (Ma *et al.*, 2021; Raga *et al.*, 2021; Navinya *et al.*, 2020; He *et al.*, 2019; Buchard *et al.*, 2017).

The reanalysis data of MERRA-2 was used to assess the effect of lockdown due to COVID-19 on the concentrations of PM_{10} and $PM_{2.5}$ over six megacities. The data of aerosols simulated by MERRA-2 were downloaded from (https://disc.gsfc.nasa.gov/), as a daily average from January 2000 to June 2020, with a spatial resolution of 0.5° lat, 0.625° long, including dust (DU) with five bins (0.1–1, 1–1.8, 1.8–3, 3–6, and 6–10 µm) (Veselovskii *et al.*, 2018), and the sea salt (SS) with five bins (0.03–0.1, 0.1–0.5, 0.5–1.5, 1.5–5, and 5–10 µm). In addition to sulfate (SO_4), black carbon hydrophilic and hydrophilic (BC1 and BC2, respectively), and organic carbon hydrophilic and hydrophilic (OC1 and OC2, respectively) (Navinya *et al.*, 2020; Provençal *et al.*, 2017). Moreover, hourly measurements of PM_{10} over Cairo were obtained from the WMO-GAW World Data Centre for Aerosols (WDCA), which are available at https://ebas.nilu.no/, while measurements over Tehran were obtained by personal communication.

MERRA-2 is a cross-track scanning instrument that provides regular global coverage of measurements.

The concentrations of PM_{10} and $PM_{2.5}$ have been calculated using equations 1 and 2, as mentioned in (https://gmao.gsfc.nasa.gov/reanalysis/MERRA-2/FAQ/).

$$PM_{10}\,(\mu g\,m^{-3}) = (SO_4 \times 1.375 + SS1 + SS2 + SS3 + SS4 + DU1 + DU2 + DU3 + DU4 \times 0.74 + (OC1 + OC2) \times 1.8 + (BC1 + BC2) \times 1e9 \quad \text{(Eq. 1)}$$

$$PM_{2.5}\,(\mu g\,m^{-3}) = (SO_4 \times 1.375 + SS2.5 + DU2.5 + (OC1 + OC2) \times 1.8 + (BC1 + BC2) \times 1e9 \quad \text{(Eq. 2)}$$

Where SS2.5 and DU2.5 are the sea salt and dust particles with a size of less than 2.5 µm, and the factor of 1.8 accounts for the conversion of organic carbon into organic matter. The sulphate concentration used for these calculations is assumed to be primarily present in the form of neutralized ammonium sulphate since the GOCART tracer is the mass of the sulphate ion, therefore, it was multiplied by a factor of 1.375 (Ukhov *et al.*, 2020).

Regression analysis was used to measure the strength of the relationship between MERRA-2 and surface observation of PM_{10} and $PM_{2.5}$.

3. RESULTS AND DISCUSSION

3.1 Monthly Means of PM during the Period 2010–2019

Fig. 1 shows the monthly means of PM_{10} and $PM_{2.5}$ concentrations over the six megacities during the period 2010–2019, extracted from MERRA-2. This figure can illustrate how MERRA-2 can represent the temporal variations of the particulate matter concentrations, which resulted from various sources and are affected by different meteorological factors.

3.1.1 Cairo

The highest concentrations of PM_{10} over Cairo, based on MERRA-2, were recorded in January and February 2020 with values exceeding 160 μg m^{-3} followed by levels that were recorded during March and December with approximately 140 μg m^{-3} (Fig. 1a). On the other hand, the lowest concentrations were observed during the summer season (June to August) with values ranging from 60 to 95 μg m^{-3}, which are consistent with the results of Mostafa *et al.* (2018). The monthly distribution of $PM_{2.5}$ followed the same pattern as PM_{10}, the highest concentrations of $PM_{2.5}$ (40 μg m^{-3}) were recorded during winter (December to February), while the lowest concentrations were recorded during the summer of the same period with values lower than 40 μg m^{-3} (Fig. 1a).

The increase in particulate concentrations during the winter months is attributed to the state of atmospheric stability and the temperature inversions that increase during the winter season (December, January, and February) in Cairo, especially during the night periods (Abou El-Magd and Zanaty, 2021; Mostafa *et al.*, 2018). The other peaks in the Spring months (March, April, and May) are due to the frequent dust storms that occur in this season because of the Khamasin depressions, which are associated with strong hot and dry winds carrying with dust and sand that increase PM_{10} and $PM_{2.5}$ concentrations over many regions in Egypt (Abou El-Magd *et al.* 2016; Incecik and Im, 2012).

3.1.2 Tehran

Fig. 1b shows the monthly distributions of PM_{10} and $PM_{2.5}$ over Tehran. The highest concentrations of PM_{10} were observed from April to July (80–85 μg m^{-3}), while, the lower concentrations were observed in December and January with (30–40 μg m^{-3}). The monthly distribution of $PM_{2.5}$ has the same behavior as PM_{10}, where April–July had high levels (more than 25 μg m^{-3}), while, November to January had lower levels (14–20 μg m^{-3}). Yousefan *et al.* (2020) attributed the high concentrations of particulate matter recorded during May to July months to the dust storms that occur during these months which are responsible for the peak concentrations of PM during summer in Tehran. Recently, Ravindra *et al.* (2022) stated that the natural emission due to dust storms during the summers causes a significant increase the concentrations of particulate matter.

3.1.3 Beijing

The highest concentrations of PM_{10} and $PM_{2.5}$ over Beijing are close to each other during the seasons of the year (Fig. 1c). The highest PM_{10} and $PM_{2.5}$ concentrations occur during the months of the summer and then fall with values ranging between 60–65 μg m^{-3}, and 53–58 μg m^{-3}, respectively. When temperatures and humidity rise, winds contribute to smog during the transport of pollutants from southern industrial areas in a warm temperate (Molina *et al.*, 2004). Whereas, the lower concentrations of PM_{10} levels were recorded during the winter months with a value of 50 μg m^{-3}, and The lower concentrations of $PM_{2.5}$ were recorded during January–April with concentrations ranging between 40-44 μg m^{-3}. These results are in agreement with the results recorded in China (Bauwens *et al.*, 2020).

3.1.4 Delhi

Reanalysis of MERRA-2 data showed that the highest concentrations of PM_{10} over Delhi were recorded from May to July (150–200 μg m^{-3}) followed by levels that recorded during October to December (120–150 μg m^{-3}) (Fig. 1d). On the other hand, the lower concentrations were observed during February, March, and September (70–90 μg m^{-3}). The highest concentrations of $PM_{2.5}$ were recorded in November and December (106 μg m^{-3} and 90 μg m^{-3}, respectively). On the other hand, the lower concentrations were observed to occur in the summer months around 50 μg m^{-3} (Fig. 1d). The high levels of PM_{10} and $PM_{2.5}$ during the summer months are because of the strong dust storms carrying large amounts of windblown dust from the desert and after this period of the dust storms the rainfall is accompanied by the monsoon season from July to September which reduces levels of $PM_{2.5}$ (Molina *et al.*, 2004). However, in the winter season, the strong surface inversions and fog cases over Delhi decrease the ability of the atmosphere to dilute the high polluted emissions (Chhikara and Kumar, 2021).

3.1.5 Mumbai

Fig. 1e shows that the highest concentrations of PM_{10} over Mumbai occurred during the summer (June and July) with concentrations of 135 and 145 μg m^{-3}, respectively. There was a drastic reduction, in August, where levels reached lower than 90 μg m^{-3}. Moreover, the lower concentrations were observed during winter (December and January) with an average of about 55 μg m^{-3}. The

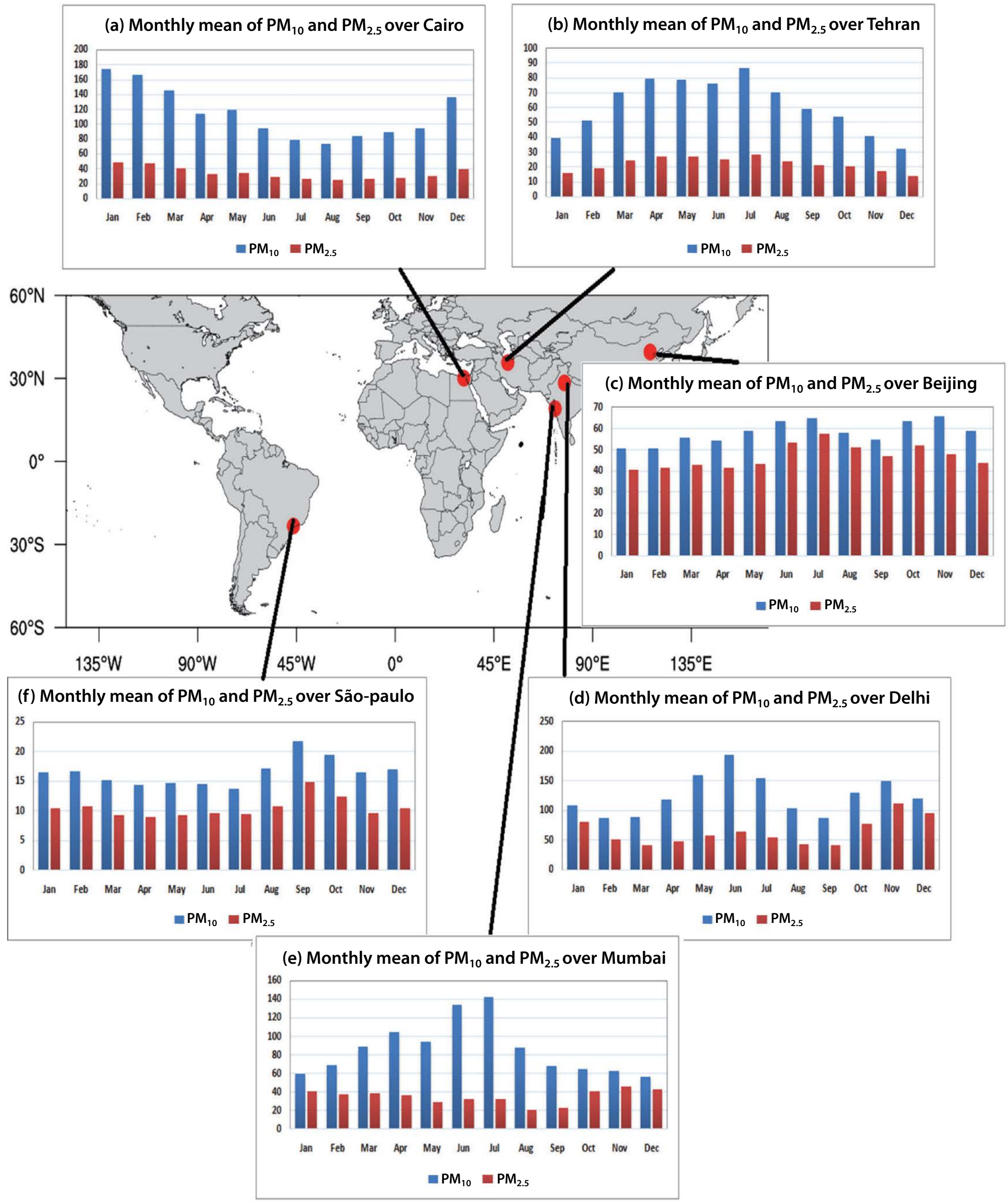

Fig. 1. Monthly mean of PM_{10} and $PM_{2.5}$ concentrations ($\mu g\ m^{-3}$) over (a) Cairo, (b) Tehran, (c) Beijing, (d) Delhi, (e) Mumbai, and (f) São-Paulo extracted from MERRA-2 during the period from January 2010 to Dec 2019 (Blue bars represent PM_{10} and the red bars represent $PM_{2.5}$).

highest concentrations of $PM_{2.5}$ were recorded during November and December to more than 40 $\mu g\ m^{-3}$, while the lower concentrations were observed during in August (about 20 $\mu g\ m^{-3}$). The reduction of PM_{10} and $PM_{2.5}$ in August could be due to the rainfall associated with the monsoon (Chhikara and Kumar, 2020; Gupta *et al.*, 2020).

3.1.6 São Paulo

Fig. 1f shows that the highest concentrations of PM_{10}

over São Paulo, were observed during the months from August to October with values ranging between 17–22 μg m^{-3}, which are accompanied by the season of lower precipitation (Nakada and Urban, 2020). On the other hand, the lower concentrations were observed during April and May (about 10 μg m^{-3}). The highest $PM_{2.5}$ concentrations were happened during September (15 μg m^{-3}), while, the lower concentrations were observed during March–May (less than 10 μg m^{-3}).

3.2 Changes in PM_{10} and $PM_{2.5}$ Levels due to COVID-19

The changes in the monthly mean of PM_{10} and $PM_{2.5}$ concentrations during COVID-19 lockdown over the megacities during January–June 2020, based on MERRA-2, are illustrated in Fig. 2. In addition, Fig. 3 shows the changes that occurred in levels of PM_{10} and $PM_{2.5}$ during the lockdown period compared to the same period in the previous 10 years (2010–2019). Tables 2 and 3 summarize the results of the mean concentrations of PM_{10} and $PM_{2.5}$, respectively, during the lockdown period and with their percentage changes compared to 2019 and the average of 2010–2019.

3.2.1 Cairo

Fig. 2a shows that the monthly average concentrations of PM_{10} in January, February, and March 2020 were 109, 96 μg m^{-3}, and 160 μg m^{-3}, respectively. The increase in concentrations in March could be ascribed to the frequent dust events that occurred during that month. The monthly average concentration was decreased from April to June, with the lowest concentrations recorded in May 2020 (83.2 μg m^{-3}), when the full lockdown applied for some consecutive days. Similarly, the monthly mean of $PM_{2.5}$ (the red line) was increased in March 2020 to approximately 45 μg m^{-3}, and then decreased after that reaching 25.8 μg m^{-3} in June by the end of the partial lockdown.

Table 2 shows that the monthly average of PM_{10} during the period from the beginning of March to the end of June 2020 in Cairo was about 109 μg m^{-3}, which is lower than the concentrations recorded in 2019 and the past ten years by about 7% and 8%, respectively. The average $PM_{2.5}$ concentration was around 32 μg m^{-3} during the same months, which is lower than the concentrations for 2019 and 2010–2019 by about 0.1% and 7%, respectively (Table 3). The reductions in the concentrations of PM_{10} and $PM_{2.5}$ over Cairo compared to 2010–2019 are illustrated in Fig. 3a (the top and bottom panels, respectively).

3.2.2 Tehran

The average concentrations of PM_{10} over Tehran were 30 and 90 μg m^{-3}, and that of $PM_{2.5}$ was 10 μg m^{-3} and 30 μg m^{-3} in January April, respectively (Fig. 2b). The lockdown in Tehran was implemented from the beginning of January to the end of February 2020. Surprisingly, due to that time, there was a slight, but insignificant, increase (2.5%) in levels PM_{10} compared to 2019, however, there was a slight reduction (4.5%) in the concentrations of $PM_{2.5}$ compared with the same period in 2019 (Tables 2 and 3). Moreover, the reductions in the levels PM_{10} and $PM_{2.5}$ were 5% and 1%, respectively, when compared to the previous ten years (Fig. 3). Surprisingly, changes in PM concentrations in Tehran were substantially smaller than the other cities. These marginal variations in $PM_{2.5}$ and PM_{10} during lockdown could be attributed to relaxation given to government offices to operate. Moreover, the lockdown was enforced for few weeks, only, in contrast to other cities which enforced the lockdown for months. Therefore, the difference was less remarkable in Tehran, than that observed in cities with the full lockdown (Lam *et al.*, 2022).

Table 2. Mean PM_{10} concentrations (μg m^{-3}) during the period of lockdown in the selected megacities, and the percentage changes in the levels compared with levels recorded in 2019 and in the previous 10 years (2010–2019). Data extracted from MERRA-2.

Megacity	Timing of lockdown in 2020	Average Level of PM_{10} during the lockdown period	Percentage change compared to 2019	Percentage change compared to the previous 10 years
Cairo	Mar–Jun	108.8	−7.45	−7.76
Delhi	Mar–Apr	74.92	−20.9	−27.3
Mumbai	Mar–Apr	86.01	−14.2	−11.2
Beijing	Feb–Apr	45.24	−1.37	−14.9
Tehran	Jan–Feb	38.90	2.45	−0.54
São Paulo	Mar–Apr	13.42	−15.42	−9.01

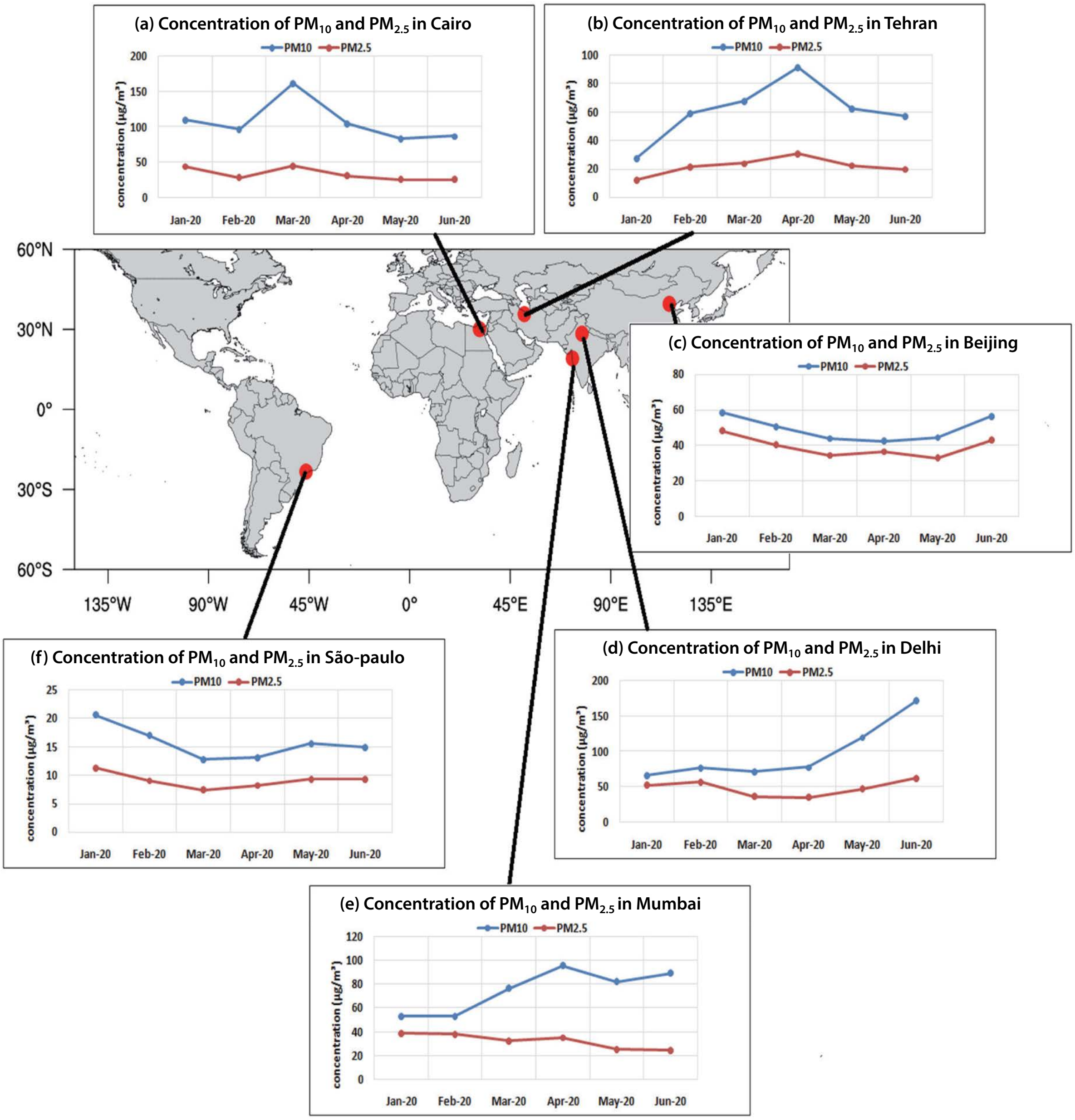

Fig. 2. Monthly mean of PM_{10} and $PM_{2.5}$ concentrations ($\mu g\ m^{-3}$) over (a) Cairo, (b) Tehran, (c) Beijing, (d) Delhi, (e) Mumbai, and (f) São-Paulo extracted from MERRA-2 during the period from January 2020 to June 2020 (Blue line represents PM_{10} and the red line represents $PM_{2.5}$).

3.3.3 Beijing

Fig. 2c shows that the average concentrations of PM_{10} and $PM_{2.5}$ over Beijing during January–June 2020. The concentrations of PM_{10} were 58.69 $\mu g\ m^{-3}$, 50.73 $\mu g\ m^{-3}$, 45 $\mu g\ m^{-3}$ and 43 $\mu g\ m^{-3}$ and the concentrations of $PM_{2.5}$ were 48.2 $\mu g\ m^{-3}$, 42.1 $\mu g\ m^{-3}$, 34.29, and 35 $\mu g\ m^{-3}$ in January, February, March, and April, respectively.

The lockdown in Beijing was implemented from the beginning of February to the end of April 2020 (Tables 2 and 3). The average concentrations of PM_{10} and $PM_{2.5}$ during these months are lower than the levels observed in 2019 by less than 2% (Table 3). Moreover, the concentrations observed in 2020 were lower than those recorded in the previous 10 years (2010–2019) by 15% and 12%, respectively (Fig. 3).

In 2020, the overall economic situation, and social and

Table 3. Mean $PM_{2.5}$ concentrations ($\mu g\ m^{-3}$) during the period of lockdown in the selected megacities, and the percentage changes in the levels compared with levels recorded in 2019 and in the previous 10 years (2010–2019). Data extracted from MERRA-2.

Megacity	Timing of lockdown in 2020	Average level of $PM_{2.5}$ during the lockdown period	Percentage change compared to 2019	Percentage change compared to the previous 10 years
Cairo	Mar–Jun	32.14	−0.09	−6.98
Delhi	Mar–Apr	36.34	−14.04	−19.63
Mumbai	Mar–Apr	33.90	−8.7	−10.47
Beijing	Feb–Apr	35.11	−1.93	−11.71
Tehran	Jan–Feb	16.80	−4.08	−1.00
São Paulo	Mar–Apr	7.85	−17.75	−14.12

economic (e.g. transportation and industrial production) activities were fully suspended in Beijing to control the COVID-19 epidemic, leading to a rapid reduction in the emission of air pollutants from vehicle exhaust and industrial production. During the epidemic control period, the significant decrease in human activity, especially the sharp reduction in traffic emissions (more than a 70% reduction compared with the same period in former years), led to a reduction in primary emissions of particulate matter (Yin *et al.*, 2021). On the other hand, pollutant discharge levels in the Beijing from 2013–2019 were higher than in 2020 (Guo *et al.*, 2021). Air quality is mainly affected by air pollution emissions and meteorological conditions. China began to significantly promote actions by which to control air pollution since 2013 (Guo *et al.*, 2021). With the implementation of the clean air policy in the Beijing, significant declines in the concentrations of $PM_{2.5}$ and PM_{10} occurred from 2013 to 2019. This could explain why the change between 2020 and 2019 were substantially smaller than that between 2020 and 2010–2019 (Delgado-Bonal *et al.*, 2020). Another explanation could be the increase in frequency of dusty weather where several dusty weather events occurred from between 2010–2019 exceeded the total of the same period in 2020 (Yin *et al.*, 2021). Moreover, the Spring Festival was suspended in 2019 (to the implementation of the clean air policy in Beijing) and 2020 (due to the lockdown), while it was carried out in the previous years (i.e. 2020–2018). These results indicate the air quality during 2020 was obviously improved compared with the same period between 2010–2019.

3.3.4 Delhi

The average concentrations of PM_{10} were 76.42 $\mu g\ m^{-3}$ and 77.53 $\mu g\ m^{-3}$, while those of $PM_{2.5}$ were 52.5 $\mu g\ m^{-3}$, 56.85 $\mu g\ m^{-3}$ in January and February 2020, respectively (Fig. 2d). These concentrations were significantly reduced after enforcement of the lockdown during March and April; where the average concentrations of PM_{10} were 72.09 $\mu g\ m^{-3}$ and 74.76 $\mu g\ m^{-3}$ in March and April 2020. Similarly, average concentrations of $PM_{2.5}$ were 37.09 $\mu g\ m^{-3}$, and 35.58 $\mu g\ m^{-3}$ in these two months, respectively (Fig. 2d).

As illustrated in Tables 2 and 3, the concentrations of PM_{10} and $PM_{2.5}$ that were observed during the lockdown in 2020 were reduced by about 21% and 14%, respectively, compared to the concentrations recorded in the same period in 2019, and by about 27%, and 20%, respectively, compared to the average duration of the last ten years, respectively, as shown in Fig. 3.

3.3.5 Mumbai

Fig. 2e shows the average concentration of PM_{10} over Mumbai during January and February were 53 $\mu g\ m^{-3}$ for both months, and during March and April (lockdown months) they were 77 $\mu g\ m^{-3}$ and 96 $\mu g\ m^{-3}$, respectively. The average concentration of $PM_{2.5}$ during January and February was around 38 $\mu g\ m^{-3}$ for both months, and were 32.5 $\mu g\ m^{-3}$ and 35.2 $\mu g\ m^{-3}$ in March and April, respectively.

Tables 2 and 3 illustrate that levels of PM_{10} and $PM_{2.5}$ over Mumbai, during the lockdown (March–April 2020), were reduced by about 14% and 9%, respectively when compared with the concentrations recorded in the same period in the previous year (2019), and by about 11% and 10% as compared to the average concentrations recorded during the same period in the previous ten years (2020–2019), respectively (Fig. 3).

3.3.6 São-Paulo

The average concentrations of PM_{10} over São Paulo were 20.64 and 17.04 $\mu g\ m^{-3}$ during January and Febru-

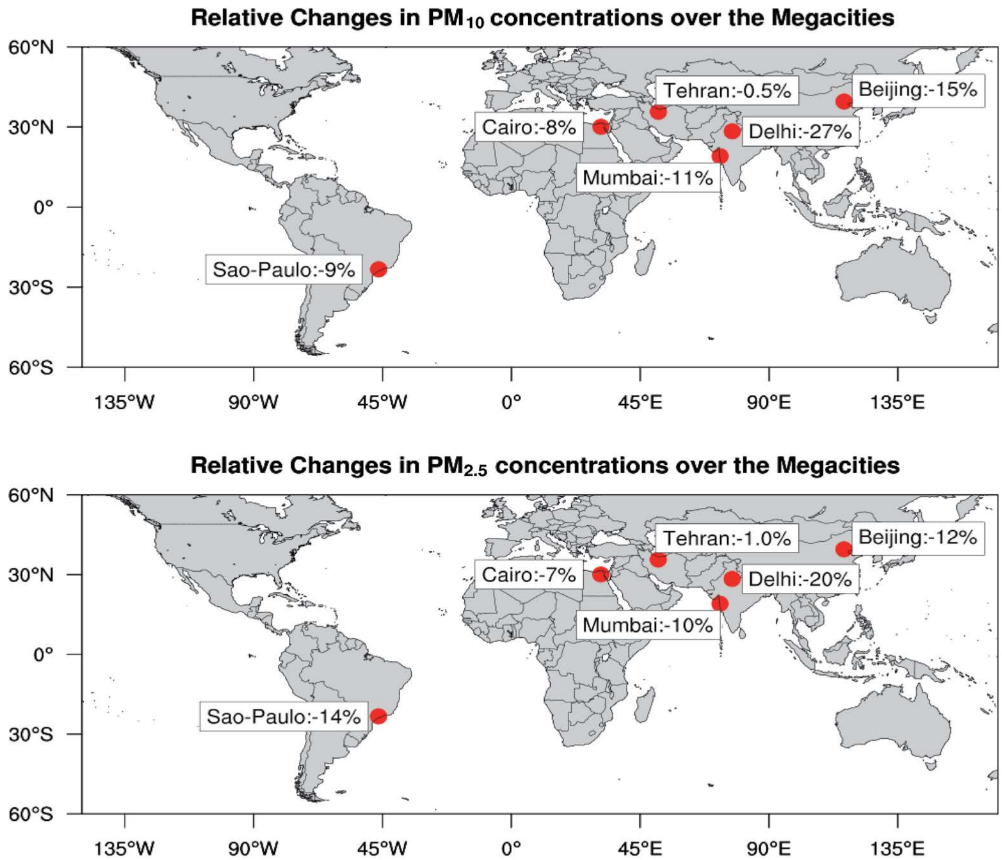

Fig. 3. Relative changes of PM_{10} (top panel) and $PM_{2.5}$ (bottom panel) occurred during the lockdown of each city in unit (%), with respect to the last 10 years (2010–2019) extracted from MERRA-2.

ary, respectively. However, during the lockdown period (March and April 2020), its concentration was 13 μg m^{-3} (Table 2).

Table 3 shows that the average concentrations of $PM_{2.5}$ during January, February, March and April were 11 μg m^{-3}, 9 μg m^{-3}, 7 μg m^{-3} and 8 μg m^{-3}, respectively. The lowest concentrations of PM_{10} and $PM_{2.5}$ were recorded in March 2020 when the full lockdown was enforced. Moreover, these concentrations were lower than those recorded in 2019 and 2010–2019 (Tables 2 and 3). There were reductions in The concentrations of PM_{10} and $PM_{2.5}$ were reduced by about 15% and 9%, when compared with the same period in 2019, and by 18% and 14%, as compared to the average duration of the previous ten years (2010–2019), respectively (Fig. 3).

Table 4 shows the comparison between PM_{10} observations at two location: the Egyptian Meteorological Authority in Cairo (Egypt) and Sherif University in Tehran (Iran) with the values extracted from MERRA-2 at the same locations during the period of 2012–2014.

Table 4. Statistical comparison for PM_{10} observations between ground stations and MERRA-2 for Cairo (Egypt) and Tehran (Iran) during the period of 2012–2014. RMSE means root mean square error.

Statistics	Site	
	Cairo	Tehran
RMSE	121.8	68.9
Correlation	0.82	0.61
Mean bias	−3.1	−4.9
Absolute percentage error	−5.58%	−13.1%

The statistical analysis of the measurements of PM_{10} concentration with the values extracted from MERRA-2 during 2012–2014 shows that the root mean square error (RMSE) was 122 and 69 μg m^{-3} for Cairo and Tehran, respectively, indicative of the reliability of the retrieved results. Also, there was a high correlation between

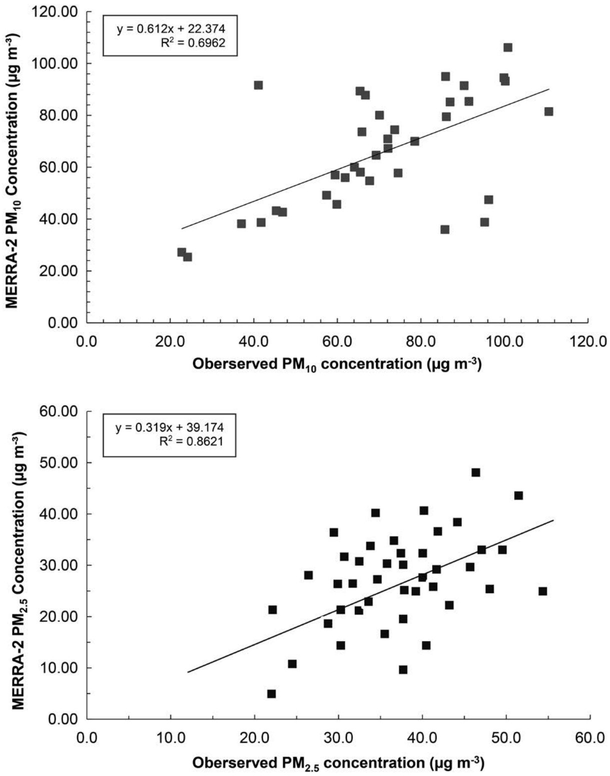

Fig. 4. Regression analysis between MERRA-2 dataset and surface observation of PM_{10} (Top panel) and $PM_{2.5}$ (lower panel). The small squares indicate the monthly mean of PM (2018–2020). The solid line is the line of best fit.

MERRA-2 and PM_{10} measurements at Cairo 0.82 with a mean bias of −3.1 μg m^{-3}, and the absolute percentage error of −5.6%, showing the applicability of the MERA-2 The results of Tehran were near to those of Cairo since the correlation is about 0.6 and the mean bias is −4.9 μg m^{-3}.

Fig. 4 shows the scatter plots and linear regressions between each reanalysis datasets obtained from MERRA-2 versus ground-based observations of PM_{10} and $PM_{2.5}$ for Cairo during 2018–2020. The results showed significant spatial agreement between MERRA-2 and ground-based observations ($R^2 = 069$ and 0.86 for PM_{10} and $PM_{2.5}$, respectively, $P < 0.05$). These results confirm the results of Table 3, and could depict that there is an agreement between MERRA-2 and ground-based observations on the global scale with a reasonable degree of accuracy (Lam *et al.*, 2022; Navinya *et al.*, 2020).

Generally, Spatiotemporal analysis of the variations in the levels of criteria air pollutants revealed that there was a significant decline in the concentration of PM_{10} and $PM_{2.5}$ in the megacities under examination. However, the magnitude of the decline in air pollutant concentrations is different in all the megacities and this is in agreement with the results of Jain and Sharma (2020). However, when compared with the WHO standards (for $PM_{2.5} = 25$ μg m^{-3}, $PM_{10} = 50$ μg m^{-3} based on a 24-hours average), Tehran and São Paulo are within the permissible limits for $PM_{2.5}$; whereas all the megacities violate WHO standards. Similarly, when compared in terms of PM_{10} levels, Cairo violates WHO standards, while other megacities are within the permissible limits.

In summary, during and after the COVID-19 pandemic, there should be a concern for environmental protection and preservation. There could be an increased population movement for environmental actions such as clean air and water (Ravindra *et al.*, 2022). Furthermore, Hassan *et al.* (2022) also linked COVID-19 pandemic with positive impact (clean beaches) and negative aspects (e.g. increase in household waste, reduced recycling).

4. CONCLUSION

In conclusion, the impact of the short-term controlled measures empowered by different governments due to the COVID-19 pandemic helped in improving air quality over the megacities, which was proved by high-resolution reanalysis data. However, the reduction in emissions of particulate matter was not significant in all cases as the lockdown was partial. Moreover, the spatial dispersion of particulate matter varied with the geographical location and the time of the year as well as meteorological parameters, and/or long-range transport of pollutants. Furthermore, these reductions are evident not only from the comparison of PM concentrations before and during the lockdown but also when comparing levels of PM observed in 2020 with those during the same period in 2019 and in the previous 10 years. Through this study, the MERRA-2 reanalysis dataset has captured the changes in PM_{10} and $PM_{2.5}$ during the short period of lockdown in different cities around the world, and thus it could be a vital tool in air quality studies in places with a lack of In-situ observations. Therefore, it is concluded that satellite-retrieved aerosol maps provide the possibility and capability of monitoring and characterizing spatiotemporal distribution of the surface PM with a reasonable degree of accuracy.

This decline in the concentration levels of PM and consequently improvement in air quality in the examined megacities could be attributed to the complete travel lockdown and suspension of all the non-essential travel activities in all the cities. Moreover, meteorology also played an essential role in the dispersion of air pollutants in all the megacities. A potential challenge is the degradation in air quality, probably to higher levels than the business-as-usual scenario attributable to increased usage of private modes of transportation in comparison to public transport due to the perception about the public transport in terms of lack of safety due to COVID-19 infection and less management by the agencies in terms of proper sanitization. This problem could be easily solved by implementation of 'odd-even' strategy for work offices and private vehicles, a quick transition from fossil fuels-based energy system to renewable and cleaner energy alternatives, plantation of trees with high surface area to volume ratio in the pollution hotspot areas, and regulating construction and demolition activities in urban areas.

This study is beneficial to the policymakers, epidemiologists, and environmentalists to access and analyze the effect of various factors on improving air quality so that future infrastructure and strategy can the planned accordingly. Integrated planning that caters to the environment and economy together came out as an essential suggestion from the experts, and they also highlighted to align all the policy decisions in line with the Sustainable Development Goals (SDGs). Modeling is urgently needed to identify the health measures and other contributing factors. In summary, the present study highlighted the importance of reductions in emissions of PM in improving air quality and this was clear during the lockdown, throughout the world. Moreover, as a blessing in disguise, it indicates that the environment is self-healing during the lockdown.

ACKNOWLEDGEMENT

We are indebted to Professor Anne McFerlane, University of Leeds for her critical revising this manuscript. This Project was funded by a generous Fund from Egyptian academy of Scientific Research & Technology (ASRT) to Ibrahim Hassan. Authors would like to acknowledge the GMAO at NASA GSFC for providing the MERRA-2 dataset, the WMO-WDCA (http://ebas-data.nilu.no/) for providing the PM_{10} observations over Cairo, and Dr. Saviz Sehat from ASMERC for providing the PM_{10} data of Sherif University in Tehran. We are indebted to anonymous reviewers for their invaluable comments.

CONFLICT OF INTEREST

The authors declare that they have no conflict of interest.

All data generated or analysed during this study are included in this published article.

REFERENCES

Abou El-Magd, I., Zanaty, N. (2021) Impacts of short-term lockdown during COVID-19 on air quality in Egypt. The Egyptian Journal of Remote Sensing and Space Sciences, 24(3), 493–500. https://doi.org/10.1016/j.ejrs.2020.10.003

Abou El-Magd, I., Zanaty, N., Ali, E.M., Irie, H., Abdelkader, A.I. (2020) Investigation of aerosol climatology, optical characteristics and variability over Egypt based on satellite observations and in-situ measurements. Atmosphere 11, 714–719. https://doi.org/10.3390/atmos11070714

Abou El-Magd, I., Ismail, A., Zanaty, N. (2016) Spatial variability of urban heat islands in Cairo City, Egypt using time series of Landsat satellite images. International Journal of Advanced Remote Sensing and GIS, 5, 1618–1638. https://doi.org/10.23953/cloud.ijarsg.48

Basahi, J., Ismail, I., Hammam, E., Hassan, I.A. (2017) Total suspended particulate matter (TSP) and its associated heavy metals in atmosphere on the Western Coast of Saudi Arabia. Polish Journal of Environmental Studies, 26(5), 2419–2424. https://doi.org/10.15244/pjoes/69102

Bashir, M.F., Jiang, M.A., Komal, B.K., Bashir, M.A., Farooq, T.H., Iqbal, N., Bashir, M. (2020) Correlation between environmental pollution indicators and COVID-19 pandemic: A brief study in Californian context. Environmental Research, 187, 109652. https://doi.org/10.1016/j.envres.2020.109652

Bauwens, M., Compernolle, S., Stavrakou, T., Müller, J.-F., Gent, J., Eskes, H., Levelt, P., Veefkind, J., Vlietinck, J., Yu, H., Zehner, C. (2020) Impact of coronavirus outbreak on NO_2 pollution assessed using TROPOMI and OMI observations. Geophysical Research Letters, 47(11). https://doi.org/10.1029/2020GL087978

Bera, B., Bhattacharjee, S., Shit, P.K., Sengupta, N., Saha, S. (2020) Significant impacts of COVID19 lockdown on urban air pollution in Kolkata (India) and amelioration of environmental health. Environment, Development and Sustainability, 23, 6913–6940. https://doi.org/10.1007/s10668-020-00898-5

Bosilovich, Michael, Cullather, Richard & National Center for Atmospheric Research Staff (Eds). Last modified September 13, 2019. "The Climate Data Guide: NASA's MERRA2 reanalysis." Retrieved from https://climatedataguide.ucar.edu/

climate-data/nasas-merra2-reanalysis

Buchard, V., Randles, C.A., da Silva, A.M., Darmenov, A., Colarco, P.R., Govindaraju, R., Ferrare, R., Hair, J., Beyersdorf, A.J., Ziemba, L.D., Yu, H. (2017) The MERRA-2 Aerosol Reanalysis, 1980 Onward. Part II: Evaluation and Case Studies. Journal of Climate, 30(17), 6851–6872. https://journals.ametsoc.org/view/journals/clim/30/17/jcli-d-16-0613.1.xml

Chhikara, A., Kumar, N. (2020) COVID-19 Lockdown: Impact on Air Quality of Three Metro Cities in India. Asian Journal of Atmoshpheric Environment, 14(4), 378–393. https://doi.org/10.5572/ajae.2020.14.4.378

COVID-19 Air Quality REPORT 2019: coronavirus pandemic lockdowns result in unprecedented reductions in deadly particle pollution. Publication date: April 22, 2020 (https://www.svlw.ch/images/aktuell/2020/REPORT-COVID-19-Impact-on-Air-Quality-in-10-Major-Cities_V5.pdf)

Delgado-Bonal, A., Marshak, A., Yang, Y., Holdaway, D. (2020) Analyzing changes in the complexity of climate in the last four decades using MERRA-2 radiation data. Scientific Reports, 10, 922 https://doi.org/10.1038/s41598-020-57917

Dhaka, S.K., Kumar, V., Panwar, V., Dimri, A.P., Singh, N., Patra, P.K., Kajino, M. (2020) $PM_{2.5}$ diminution and haze events over Delhi during the COVID-19 lockdown period: an interplay between the baseline pollution and meteorology. Scientific Reports, 10(1), 1–8. https://doi.org/10.1038/s41598-020-70179-8

Doraiswamy, P., Sarwar, G., Farnoud, A. (2017) Air quality in megacities around the world. EM Magazine, 11–22. https://www.awma.org/blog_home.asp?15

El Sheekh, M., Hassan, I.A. (2021) Lockdowns and reduction of economic activities during the COVID-19 pandemic improved air quality in Alexandria, Egypt. Environmental Monitoring and Assessment, 193(1), 11. https://doi.org/10.1007/s10661-020-08780-7

Faridi, S., Yousefian, F., Niazi, S., Ghalhari, M.R., Hassanvand, M.S., Naddafi, K. (2020) Impact of SARS-CoV-2 on ambient air particulate matter in Tehran. Aerosol and Air Quality Research, 20(8), 1805–1811. https://doi.org/10.4209/aaqr.2020.05.0225

Fattorini, D., Regoli, F. (2020) Role of the chronic air pollution levels in the Covid-19 outbreak risk in Italy. Environmental Pollution, 264, 114732. https://doi.org/10.1016/j.envpol.2020.114732

Guo, Q., Wang, Z., He, Z., Li, X., Meng, J., Hou, Z., Yang, J. (2021) Changes in air quality from the COVID to the post-COVID era in the Beijing-Tianjin-Tangshan Region in China. Aerosol and Air Quality Research, 21, 21–27. https://doi.org/10.4209/aaqr.210270

Gupta, N., Tomar, A., Kumar, V. (2020) The effect of COVID-19 lockdown on the air environment in India. Global Journal of Environmental Science and Management, 6, 31–40. https://doi.org/10.22034/GJESM.2019.06.SI.04

Haiba, N., Hassan, I.A. (2018) Monitoring and assessment of PAHs in the atmosphere of Alexandria city, Egypt. Polycyclic Aromatic Compounds, 38(3), 219–230. https://doi.org/10.1080/10406638.2016.1200102

Hassan, I.A., Younis, A., Al Ghamdi, M.A., Wahab, M., Mazroui, M., Abou Al Kher, E., Al Hussaini, M., Haiba, N., El Magraby, D. (2022) Contamination of the marine environment in Egypt and Saudi Arabia with personal protective equipment during COVID-19 pandemic: A short focus. The Science of the Total Environment, 810, 152046. https://doi.org/10.1016/j.scitotenv.2021.152046

Haque, Md. S., Singh, R.B. (2017) Air Pollution and Human Health in Kolkata, India: A Case Study. Climate, 5(4), 77–85. https://doi.org/10.3390/cli5040077

He, L., Lin, A., Chen, X., Zhou, H., Zhou, Z., He, P. (2019) Assessment of MERRA-2 Surface $PM_{2.5}$ over the Yangtze River Basin: ground-based verification, spatiotemporal distribution and meteorological dependence. Remote Sensing, 11, 460. https://doi.org/10.3390/rs11040460

Hosseini, V.,Shahbazi, H. (2016) Urban Air Pollution in Iran. Iranian Studies, 49(6), 1029–1046. https://doi.org/10.1080/00210862.2016.1241587

Incecik, S., Im, U. (2012) Air pollution in mega cities: a case study of Istanbul. Air pollution-Monitoring, Modelling and Health, InTech, pp. 77-116.

Ismail, I.M., Summan, A.S., Basahi, J.M., Hammam, E., Yasin, M.F., Hassan, I.A. (2021) First measurements of carbonaceous aerosol across urban, rural and residential areas in Jeddah city, Saudi Arabia. Asian Journal of Atmospheric Environment, 15(2), 1–14. https://doi.org/10.5572/ajae.2021.021

Jain, S., Sharma, T. (2020) Social and travel Lockdown impact considering Coronavirus disease (COVID-19) on air quality in Megacities of India: present benefits, future challenges and way forward. Aerosol and Air Quality Research, 20, 1222–1236. https://doi.org/10.4209/aaqr.2020.04.0171

Lam, Y.-F., Chang, J.M.H., Loo, B.P.Y., Zhang, H.-S., Leung, K.K.M., Axhausen, K.W. (2022) Screening approach for short-term $PM_{2.5}$ health co-benefits: A case study from 15 Metropolitan cities around the world during the COVID-19 pandemic. Atmosphere, 13, 18. https://doi.org/10.3390/atmos13010018

Lu, H., Stratton, C.W., Tang, Y-W. (2020) The Wuhan SARS-CoV-2 - What's next for China. Journal of Medical Virology, 92, 546–547. https://doi.org/10.1002/jmv.25738

Luna, M.A.G., Luna, F.A.G., Espinosa, J.F.M., Cerón, L.C.B. (2018) Spatial and Temporal Assessment of Particulate Matter Using AOD Data from MODIS and Surface Measurements in the Ambient Air of Colombia. Asian Journal of Atmospheric Environment, 12(2). https://doi.org/10.5572/ajae.2018.12.2.165

Ma, X., Yan, P., Zhao, T., Jia, X., Jiao, J., Ma, Q., Wu, D., Shu, Z., Sun, X., Habtemicheal, B.A. (2021) Evaluations of Surface PM_{10} concentration and chemical compositions in MERRA-2 aerosol reanalysis over Central and Eastern China. Remote Sensing, 13, 1317. https://doi.org/10.3390/rs13071317

Molina, L.T., Molina, M.J., Slott, R.S., Kolb, C.E., Gbor, P.K., Meng, F., Tang, X. (2004) Air quality in selected megacities. Journal of the Air & Waste Management Association, 54(12), 1–73.

Mostafa, A.N., Zakey, A.S., Monem, A.S., Wahab, M.M. (2018) Analysis of the surface air quality measurements in the greater Cairo (Egypt) metropolitan. Global Journal of Advanced

Research, 5, 207–214.
Nakada, L.Y.K., Urban, R.C. (2020) COVID-19 pandemic: Impacts on the air quality during the partial lockdown in São Paulo state, Brazil. Science of The Total Environment, 730, 139087. https://doi.org/10.1016/j.scitotenv.2020.139087
Navinya, C.D., Vinoj, V., Pandey, S.K. (2020) Evaluation of $PM_{2.5}$ Surface Concentrations Simulated by NASA's MERRA Version 2 Aerosol Reanalysis over India and its relation to the Air Quality Index. Aerosol Air Quality Research, 20, 1329–1339. https://doi.org/10.4209/aaqr.2019.12.0615
Pei, Z., Han, G., Ma, X., Su, H., Gong, W. (2020) Response of major air pollutants to COVID-19 lockdowns in China. Science of the Total Environment, 743, 140879.
Provençal, S., Buchard, V., da Silva, A.M., Leduc, R. (2017) Evaluation of PM surface concentrations simulated by Version 1 of NASA's MERRA Aerosol Reanalysis over Europe. Atmospheric Pollution, 8(2), 374-382. https://doi.org/10.1016/j.apr.2016.10.009
Raga, G.B., Ladino, L.A., Baumgardner, D., Ramirez-Romero, C., Córdoba, F., Alvarez-Ospina, H., Rosas, D., Amador, T., Miranda, J., Rosas, I., Jaramillo, A., Yakobi-Hancock, J., Kim, J.S., Martínez, L., Salinas, E., Figueroa, B. (2021) ADABBOY: African dust and biomass burning over Yucatan. Bulletin of the American Meteorological Society, 102(8), 1543–1556.
Randles, C.A., da Silva, A.M. (2017) The MERRA-2 Aerosol Reanalysis, 1980 Onward. Part I: System Description and Data Assimilation Evaluation. Journal of Climate, 30(17), 6823–6850. https://doi.org/10.1175/J.CLI-D.16-0609.1
Ravindra, K., Singh, T., Vardhan, S., Shrivastava, A., Singh, S., Kumar, P., Mor, S. (2022) COVID-19 pandemic: What can we learn for better air quality and human health?. Journal of Infection and Public Health, 15(2), 187–198. https://doi.org/10.1016/j.jiph.2021.12.001
Rohrer, M., Flahault, A., Stofel, M. (2020) Peaks of fine particulate matter May modulate the spreading and virulence of COVID19. Earth Systems and Environment, 4,789–796. https://doi.org/10.1007/s41748-020-00184-4
Shi, X., Brasseur, G.P. (2020) The response in air quality to the reduction of Chinese economic activities during the COVID-19 outbreak. Geophysical Research Letters, 47(11), e2020GL088070. https://doi.org/10.1029/2020GL088070
Ukhov, A., Mostamandi, S., da Silva, A., Flemming, J., Alshehri, Y., Shevchenko, I., Stenchikov, G. (2020) Assessment of natural and anthropogenic aerosol air pollution in the Middle East using MERRA-2, CAMS data assimilation products, and high-resolution WRF-Chem model simulations. Atmospheric Chemistry and Physics, 20(15), 9281–9310.
Veselovskii, I., Goloub, P., Podvin, T., Tanre, D., da Silva, A., Colarco, P., Castellanos, P., Korenskiy, M., Hu, Q., Whiteman, D.N. (2018) Characterization of smoke and dust episode over West Africa: comparison of MERRA-2 modelling with multiwavelength Mie-Raman lidar observations, Atmospheric Measurement Techniques, 11, 949–969. https://doi.org/10.5194/amt-11-949-2018
WHO (World Health Organization) (2020a) Novel Coronavirus disease (COVID-19) outbreak. Available from www.int/emergencies/diseases/novel-coronavirus-2019 (Accessed on 25 April 2020).
WHO (World Health Organization) (2020b) Novel Coronavirus (COVID-19) Situation report 1, 21 January 2020. www.int/docs/default-source/coronaviruse/situation-reports/20200121-sitrep-1-2019-ncov.pdf
WHO (World Health Organization) (2020c) Novel Coronavirus (COVID-19), Situation report 31, 20 February 2020. www.int/docs/default-source/coronaviruse/situation-reports/20200220-sitrep-31-covid-19.pdf (Accessed in 25 April 2020).
WHO/UNEP (1994) Air Pollution in 20 Megacities around the world. World Health Organization, United Nation Environmental, Annual report, Switzerland.
Yin, Z., Wan, Y., Zhang, Y., Wang, H. (2021) Why super sandstorm 2021 in North China. National Science Review, 9(3), nwab165. https://doi.org/10.1093/nsr/nwab165
Yousefan, F., Sasan, F., Azimi, F., Aghaei, M., Shamsipour, M., Yaghmaeian, K., Hassanvand, M.S. (2020) Temporal variations of ambient air pollutants and meteorological influences on their concentrations in Tehran during 2012–2017. Scientific Reports, 10, 292. https://doi.org/10.1038/s41598-019-56578-6